

## Acceleration-dependent lateral track resistance for the condition assessment of railway bridges with ballasted track

Ocena stanu technicznego obiektów mostowych z nawierzchnią kolejową na podsypce tłuczniowej uwzględniająca wpływ przyspieszenia poprzecznego na siłę oporu bocznego toru

**Abstract:** Lateral track resistance is essential for assessing rail track stability and the operational safety of railway lines. This contribution addresses the experimental investigation of lateral track resistance on railway bridges subjected to dynamic loads. The experiments are carried out using a large-scale test facility, replicating a representative section of a railway bridge at a scale of 1:1, thus enabling a targeted and isolated observation of the ballast superstructure's behaviour. The investigations aim to identify the influence of vertical vibrations on lateral track resistance, both for unloaded and vertically loaded track. Based on the experiments, load-dependent acceleration limits are identified, above which a significant reduction in lateral track resistance occurs. Furthermore, experimental lateral load-displacement curves depending on the vertical load and acceleration level are generated for determining lateral track stiffness. The results comprise the identified limit values for vertical accelerations and the acceleration-dependent lateral track resistances, which can be applied for condition assessment of railway bridges in the context of dynamic assessment.

**Keywords:** ballasted track, condition assessment, experiments, lateral track-bridge interaction, railway bridges.

**Streszczenie:** Opór boczny toru kolejowego jest podstawowym parametrem niezbędnym do oceny warunków utraty stateczności i bezpieczeństwa podczas eksploatacji nawierzchni kolejowej. W artykule przedstawiono wyniki badań eksperymentalnych służące do oceny siły oporu bocznego toru na mostach kolejowych poddanych obciążeniom dynamicznym. Badania przeprowadzono na pełnowymiarowym obiekcie testowym, będącym modelem fragmentu mostu kolejowego w skali 1:1, co umożliwiło obserwację warstwy podsypki tłuczniowej wyodrębnionej z konstrukcji nawierzchni kolejowej. Badania miały na celu określenie wpływu drgań poprzecznych na graniczną wartość siły oporu bocznego toru – w warunkach bez obciążenia oraz w przypadku występującego obciążenia pionowego. Na podstawie przeprowadzonych eksperymentów wyznaczono graniczne wartości przyspieszenia, powyżej których następuje znacząca redukcja siły oporu bocznego toru. W artykule zamieszczono także – wyznaczone eksperymentalnie – krzywe obciążenia poprzecznego w funkcji przemieszczenia, w zależności od rodzaju obciążenia pionowego i wartości przyspieszenia. Uzyskane w wyniku badań graniczne wartości przyspieszenia poprzecznego oraz zależne od przyspieszenia – graniczne wartości siły oporu bocznego toru można wykorzystać do oceny stanu mostów kolejowych pod kątem ich wytrzymałości na obciążenia dynamiczne.

**Słowa kluczowe:** eksperymentalna ocena stanu nawierzchni torowej, mosty kolejowe, nawierzchnia torowa na podsypce tłuczniowej, oddziaływanie poprzeczne toru z mostem.

<sup>1)</sup> TU Wien, Institute of Structural Engineering, Karlsplatz 13, A-1040 Vienna, Austria; andreas.stollwitzer@tuwien.ac.at (✉)

<sup>2)</sup> TU Wien, Institute of Structural Engineering, Karlsplatz 13, A-1040 Vienna, Austria; lara.bettinelli@tuwien.ac.at

<sup>3)</sup> TU Wien, Institute of Structural Engineering, Karlsplatz 13, A-1040 Vienna, Austria; samuel.loidl@tuwien.ac.at

<sup>4)</sup> TU Wien, Institute of Structural Engineering, Karlsplatz 13, A-1040 Vienna, Austria; josef.fink@tuwien.ac.at

## 1. INTRODUCTION

Dynamic assessment of railway bridges is essential for ensuring the compatibility between bridges and rolling stock. Most importantly, the acceleration limits for bridge vibrations due to train passage must be met to ensure operational safety. Furthermore, knowledge of the impact of dynamic excitations on the condition of the ballast superstructure is of essential importance in order to assess the stability of the track during operation.

To ensure serviceability under dynamic excitation, EN 1990/A1 [1] specifies the maximum permissible vertical acceleration of  $3.5 \text{ m/s}^2$  for newly-constructed railway bridges with ballast superstructures. At a national level in Austria, a higher limit value of  $6.0 \text{ m/s}^2$  is allowed for existing bridges according to standard B 4008-2 [2]. The restriction of the permissible limit accelerations is based on investigations on the track stability under vertical loading [3] and primarily ensures the superstructure's structural stability under dynamic excitation during operation.

Dynamic calculations of railway bridges for predicting bridge vibrations due to train crossings are mainly focused on vertical vibrations of the supporting structure and vertical interaction between track and supporting structure, see e.g. [4-7]. This contribution deals with experimental investigations of lateral track-bridge interaction, particularly the lateral track resistance (resistance transverse to the track axis) on bridges. The subject of the presented research is the manner in which the vertical vibration state, i.e. vertical accelerations of the structure due to dynamic excitation, affects the lateral track resistance (Fig. 1).

Lateral track resistance is a key indicator for assessing track stability, where excessive stresses due to temperatures (longitudinal rail stresses) as well as stresses due to horizontal loads from the vehicle (load transverse to the track axis), can lead to distortions [8-11]. The risk of loss of stability is particularly significant in curved tracks.

Lateral track resistance depends on several factors, including the used ballast, the type of sleeper, base friction between the sleepers and ballast bed, contribution of the shoulder, rail pads, and particularly the compaction condition of the ballast bed. According to [10], 45%-50% of lateral displacement resistance is provided by base friction, 35%-40% by the shoulder and 10%-15% by friction between sleeper flanks and ballast bed. Similar percentage breakdowns are also given in [12].

The dependence of lateral track resistance on several factors also causes a considerable scatter in the values of specific resistance indicators. Experimental measurements of lateral track resistance usually refer to the resistance of one single sleeper, with measurements being carried out in the open track [10, 13-14]. To define the experimentally determined lateral track resistance based on generated force-displacement curves, the force associated with the displacement of  $2.0 \text{ mm}$  is usually used for specifying a concrete value. Fig. 2 shows two possible definitions of lateral track resistance. According to Fig. 2a, the force value at  $2.0 \text{ mm}$  is used as the resistance; according to Fig. 2b, the elastic part of the deformation is considered, which can be considered in combination with corresponding release [10]. In the investigations presented in this article, the value  $P_{lat}(2.0 \text{ mm})$  according to Fig. 2a is used as the definition for the lateral track resistance (see section 3.2).

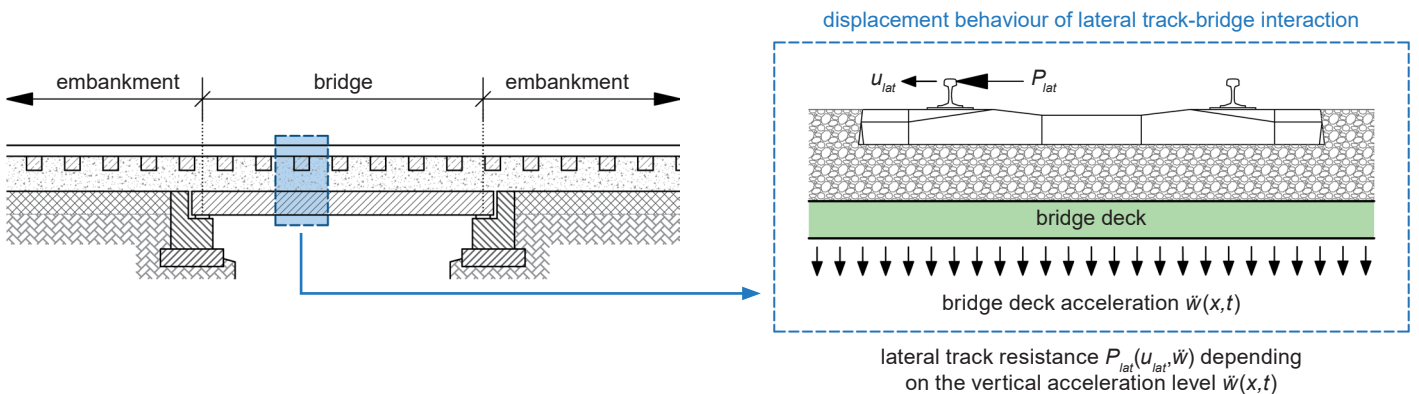


Fig. 1. Lateral track-bridge interaction in dynamically excited railway bridges with ballast superstructure

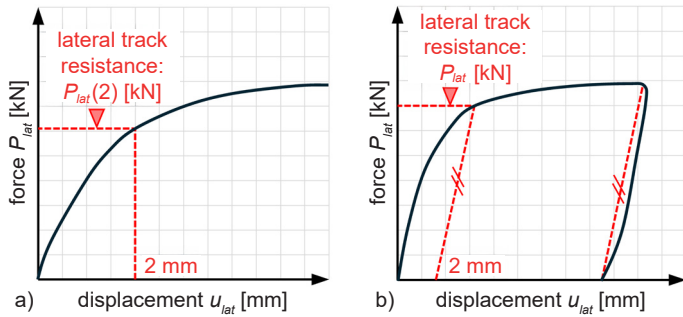


Fig. 2. Determination of lateral track resistance from experiments

The values given in the literature for the resistance  $P_{lat}$  (2.0 mm) are between 3 kN and 47 kN [10, 13-18] depending on the geometric boundary conditions, ballast material and load condition (unloaded vs vertically loaded track) and therefore vary considerably. According to [10], a resistance  $P_{lat}$  (2.0 mm) of 5-10 kN per sleeper is indicated for unloaded track. Furthermore, [6] also gives information on lateral track resistance in the form of a linear spring stiffness; in this case, longitudinal track stiffness (longitudinal displacement resistance) is equated with lateral stiffness, which corresponds to a resistance  $P_{lat}$  of 4.62 kN per sleeper (distance 0.60 m) with a defined longitudinal spring stiffness of 3.85 kN/mm per unit length of track. However, equating lateral and longitudinal track resistance is an oversimplification, as the resistances and energy dissipation depend significantly on the direction of loading (lateral vs longitudinal). Experimental analyses of longitudinal track resistance can be found in [19, 20].

Experimental and theoretical studies on lateral track resistance primarily deal with sections in the open track [8-18]. In contrast, this contribution is dedicated to an experimental assessment of lateral track resistance related to railway bridges, whereby the condition of the ballast superstructure on the bridge, which is excited to vertical vibrations, is the subject of the investigations. The primary aim of the investigations is to experimentally determine the influence of the vertical acceleration state on lateral track resistance. In this context, the extent to which the limiting accelerations defined in [1, 2] can also be applied to lateral track resistance will be discussed in particular. For the envisaged targeted investigation of lateral track resistance under dynamic excitation, a special large-scale test facility was developed at the Institute of Structural Engineering – Research Unit Steel Structures at TU Wien to enable – among other things – these investigations.

In the following sections, the test facility and its operating principle are first introduced (section 2). Furthermore, the experimental results concerning the lateral track-bridge interaction are presented (section 3).

## 2. LARGE-SCALE TEST FACILITY AND TEST PRINCIPLE

### 2.1. TEST FACILITY AT THE SCALE OF 1:1

The investigations into the dynamic characteristics of the ballast superstructure concerning lateral track resistance are part of a concluded research project at TU Wien. The investigations are carried out using a large-scale test facility, which enables targeted and isolated research into the dynamic behaviour of the ballast superstructure independently of the behaviour of the supporting structure. The test facility (Fig. 3) consists of a 7.0 m long and 2.5 m wide steel trough, in which a section of ballast superstructure at the scale of 1:1 is installed over a length of 2.4 m. The design of the steel trough replicates a typical single-track steel railway bridge and consists of two vouted main girders with a deck plate in between and transversely orientated girders (cross girders).

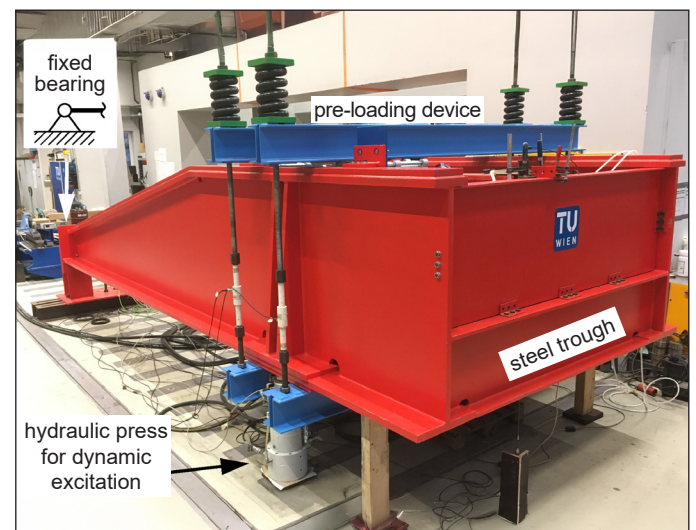


Fig. 3. Large-scale test facility

The installed section of the ballast superstructure consists of a UIC 60 rail, four halves of concrete sleepers, a 55 cm ballast bed and a sub-ballast mat; it thus corresponds to one half cross-section of a railway bridge. Fig. 4 shows a cross-section of the test facility with the section of ballast superstructure installed.

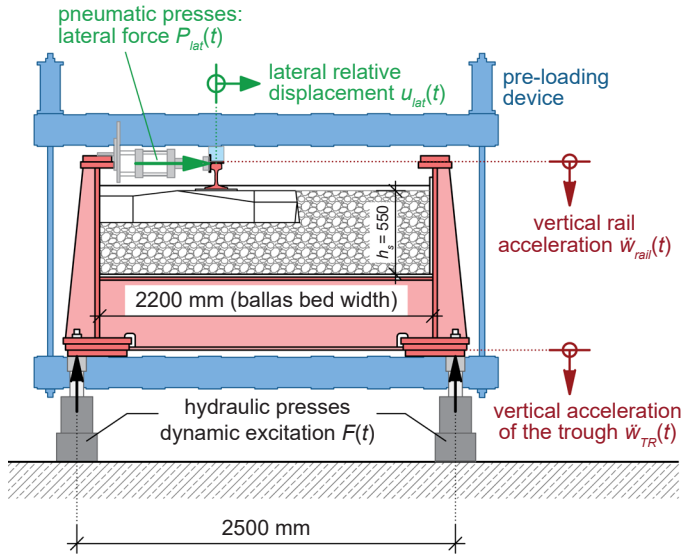


Fig. 4. Cross-section of the test facility

Concerning the functional principle of the test facility, the steel trough at one end is supported on a fixed bearing (Fig. 3), which enables rotational movement of the steel trough. Two hydraulic presses are positioned below the steel trough to apply dynamic excitation; they vertically excite the steel trough to vibrate at a predefined excitation frequency and displacement or acceleration amplitude (Figs 3 and 4). When dynamically excited by the hydraulic presses, the steel trough thus undergoes a tilting movement around the fixed bearing. It can be assumed for simplification purposes that the vertical movements of the integrated ballast superstructure are uniform, i.e. the entire ballast superstructure in the test facility has uniform vertical movement kinematics, as the section of ballast superstructure installed over a length of 2.4 m has a sufficiently large distance from the fixed support. The vertical accelerations measured in the experiments confirm this assumption [22]. Thus, figuratively speaking, a section of a ballasted track with uniform kinematics on the bridge is simulated in the experiment. Regarding the installed section of ballast superstructure, the half cross-section was selected due to the lower mass compared to a whole cross-section, which makes it possible to achieve excitation frequencies of up to 25 Hz with the existing hydraulic system. Such frequencies would not be achievable with a larger section due to the considerably higher inertial forces.

The blue steel structure which can be seen in Figs 3 and 4 is a pre-loading device. It can be forced down on the rail

at two points, making it possible to analyse not only the condition of unloaded track, but also the condition of vertically loaded track. In this case, the load applied by the pre-loading device is 125 kN, which corresponds to half the static axle load of a Railjet locomotive (250 kN). This value also corresponds to the load level for single loads according to LM 71 in EN 1991-2 [21].

## 2.2. TEST PRINCIPLE FOR QUANTIFICATION OF LATERAL TRACK RESISTANCE

In order to analyse the lateral track resistance, two pneumatic presses are arranged at the same level as the rail axis, applying a load in the lateral direction  $P_{lat}$ , as shown in Fig. 4 (marked in green) and 5.

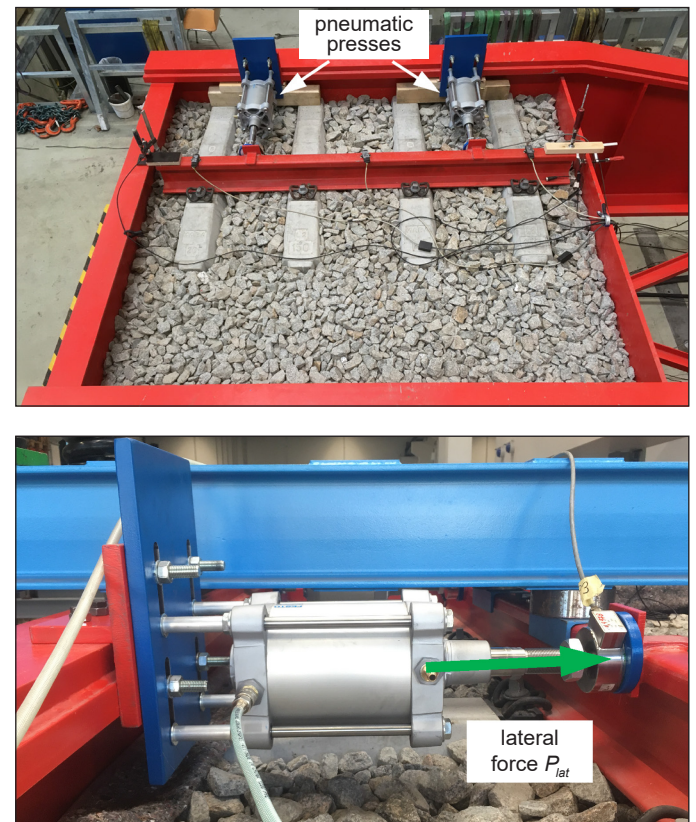


Fig. 5. Integrated ballasted track and pneumatic presses for applying lateral force

Two different test principles are used for quantifying the lateral track resistance in dependence on the vertical acceleration state – defined by the accelerations of the trough  $\ddot{w}_{TR}(t)$  and the rail  $\ddot{w}_{rail}(t)$  (Fig. 4). In principle 1, a constant force  $P_{lat}$  is applied in the lateral direction (static load in the lateral direction) and the vertical acceleration

is successively increased. This test principle is used to identify critical combinations of lateral force, vertical acceleration and excitation frequency at which a significant change in lateral track resistance occurs. This principle is primarily intended to assess whether the limit accelerations defined in [1, 2] can also be assumed to be reliable limit values concerning lateral track resistance. In principle 2, the facility is first set to a stationary vibration state, defined by excitation frequency and acceleration amplitude, and subsequently the lateral force  $P_{lat}$  is continuously increased. The aim is to determine force-displacement curves for different acceleration levels and load situations (unloaded and vertically loaded track). The two test principles are, therefore, as follows:

- principle 1: constant force  $P_{lat}$  and increasing accelerations  $\ddot{w}_{TR}$ ,  $\ddot{w}_{rail}$ ,
- principle 2: constant accelerations  $\ddot{w}_{TR}$  and  $\ddot{w}_{rail}$  and increasing force  $P_{lat}$ .

The excitation frequencies related to the two principles are between 5 Hz and 25 Hz. The total lateral force  $P_{lat}$  that can be applied is limited to 40 kN by the available pneumatic system. EN 1991-2 [21] prescribes a lateral load of 100 kN, but this applies to the static load case and is always applied in combination with a vertical load. The experimental results, which are presented in the following section, may be extrapolated to this level.

### 3. EXPERIMENTAL RESULTS

#### 3.1. ACCELERATION LIMITS

This section presents the results of the experimental investigations of lateral track resistance of vertically oscillating ballast superstructure. As mentioned in section 2, in addition to analysing lateral track resistance, the test facility also enables the experimental investigation of the vertically occurring energy dissipation mechanisms in the ballast superstructure. Experimental results concerning vertical track-bridge interaction are presented in [22, 23]. The experiments were performed using dry and non-frozen ballast bed and are considered summer tests. It should be mentioned that in the case of a frozen ballast bed (winter tests), the stiffness of the ballast bed increases significantly [19].

First, the results from principle 1 (constant force and increase in acceleration) and for the unloaded track are discussed. Tests were carried out with four different load

levels and different excitation frequencies, listed below and related to the lateral force per half-sleeper:

- load 1: 1.2 kN/half-sleeper – frequencies: 5/10/15/20/25 Hz,
- load 2: 2.1 kN/half-sleeper – frequencies: 5/10/15/20 Hz,
- load 4: 3.1 kN/half-sleeper – frequency: 15 Hz,
- load 5: 4.0 kN/half-sleeper – frequency: 5 Hz.

Fig. 6 first shows the lateral displacement  $u_{lat}$  for the unloaded track condition as a function of the vertical acceleration amplitude of the rail  $\ddot{w}_{rail}$  for all four load levels and different excitation frequencies (see legend). Based on this illustration, it is possible to identify limit states from which a significant increase in the relative displacement and, thus, a decrease in the lateral track resistance occurs. Fig. 6 shows no abrupt increases in lateral displacement at load 1 and load 2 with excitation frequencies up to 15 Hz. At load 2 and 20 Hz excitation frequency, however, there is a disproportionate increase in lateral displacement at the acceleration  $\ddot{w}_{rail}$  of around 5.5 m/s<sup>2</sup>. The same applies to load levels 3 and 4, whereby a significant increase in lateral relative displacement occurs even at comparatively lower vertical accelerations. Fig. 6 thus clearly shows that, depending on the lateral load and acceleration level, limit values can be identified (marked in red in Fig. 6) above which a significant change in the ballast superstructure occurs (as a substantial decrease in lateral track resistance).

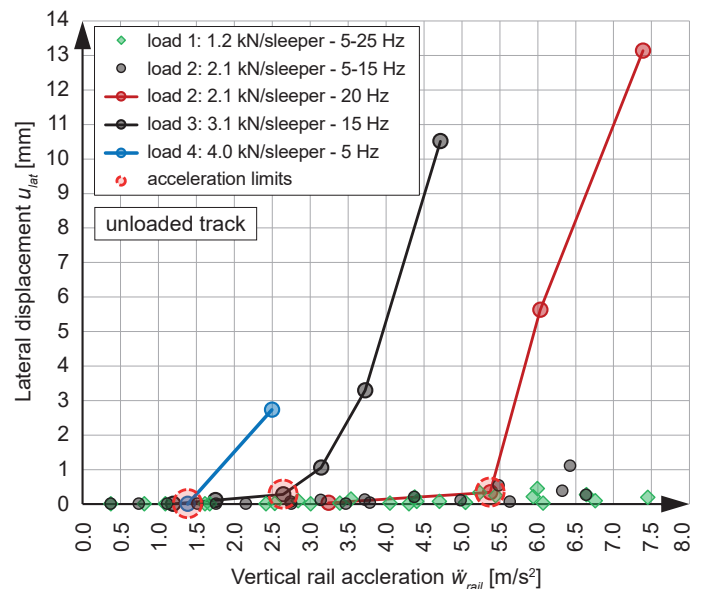


Fig. 6. Test principle 1 – lateral relative displacement depending on vertical rail acceleration for different load steps (unloaded track)

Based on the limit values marked in Fig. 6, Fig. 7 shows the limit acceleration values identified in the tests (values corresponding to the beginning of ballast bed destabilisation) as a function of the lateral load (for unloaded track). As the lateral load increases, the limit acceleration, from which a disproportionate rise in lateral track displacement occurs, decreases. In some cases, the limit accelerations are clearly below the normative limit values of  $3.5 \text{ m/s}^2$  (according to [1]) or  $6.0 \text{ m/s}^2$  (according to [2]). When the excitation frequency is neglected for the sake of simplification, a quadratic and lateral load-dependent regression function is defined to describe the limit state (red dashed line in Fig. 7):

$$\ddot{w}_{rail,lim} = 0.543 P_{lat}^2 - 5.27 P_{lat} + 13.8, [\text{m/s}^2]. \quad (1)$$

This regression function describes the identified limit acceleration and thus marks the transition from safe operating area to unsafe operating area (Fig. 7) in relation to the lateral resistance of unloaded track.

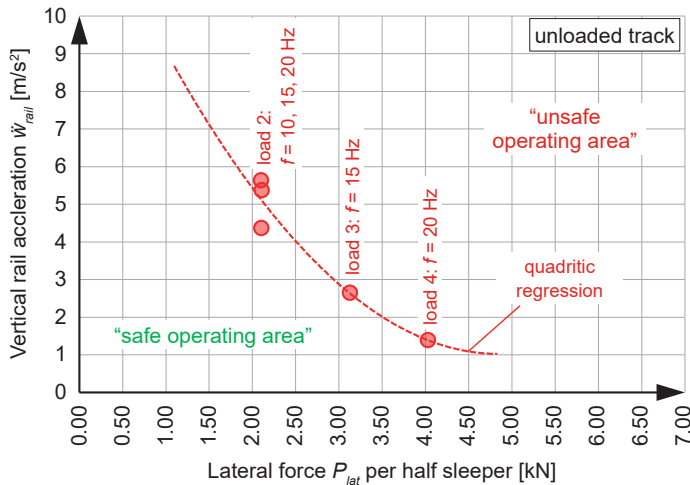


Fig. 7. Test principle 1 – load-dependent acceleration limits for lateral track resistance (unloaded track)

In addition to the experiments with unloaded track, tests with vertically loaded track were also carried out according to the same principle, whereby a total of seven load levels with lateral loads between  $0.6 \text{ kN}$  and  $9.2 \text{ kN}$  per half-sleeper ( $0.6 \text{ kN}$ ,  $1.2 \text{ kN}$ ,  $2.1 \text{ kN}$ ,  $4.1 \text{ kN}$ ,  $6.0 \text{ kN}$ ,  $8.0 \text{ kN}$  and  $9.2 \text{ kN}$ ) were used. The related excitation frequencies for all lateral load levels are  $5 \text{ Hz}$ ,  $10 \text{ Hz}$ ,  $15 \text{ Hz}$ ,  $20 \text{ Hz}$  and  $25 \text{ Hz}$ . Hence, the lateral loads for the experiments with vertically loaded track are significantly higher than those for the unloaded track.

The identification of limit states in the form of load-dependent acceleration limits is carried out for the loaded track in the same way as for the unloaded track (Figs 6 and 7). In the following, as an extension of Fig. 7, the limit accelerations identified for the loaded track are shown in Fig. 8 (blue squares) and compared with those for the unloaded track. In the case of the loaded track, significant displacements in the lateral direction only occur at a load level above  $4 \text{ kN}$  per half-sleeper (Fig. 8 – load 4). With a smaller lateral load, there is no measurable lateral loss of stiffness regardless of the vertical acceleration level, which is why the results shown in Fig. 8 only begin at lateral loads above  $4 \text{ kN}$ .

Fig. 8 shows that vertical loading of the track significantly influences its lateral resistance. Furthermore, for the loaded state, it can be seen that measurable stiffness losses in the lateral direction only occur at excitation frequencies above  $15 \text{ Hz}$ , which means that the limiting accelerations shown in Fig. 8 do not apply to the entire test range, but only to excitation frequencies above  $15 \text{ Hz}$  and loads above  $4 \text{ kN}$  per half-sleeper. In addition, the relative displacements for the loaded state, which occur with an identified loss of stiffness (defined as disproportionate increase of lateral displacement), are at a considerably lower level ( $< 2 \text{ mm}$ ) than in the unloaded state ( $3\text{-}13 \text{ mm}$ , Fig. 6). The limit values given in Fig. 8 are therefore interpreted as being considerably on the safe side.

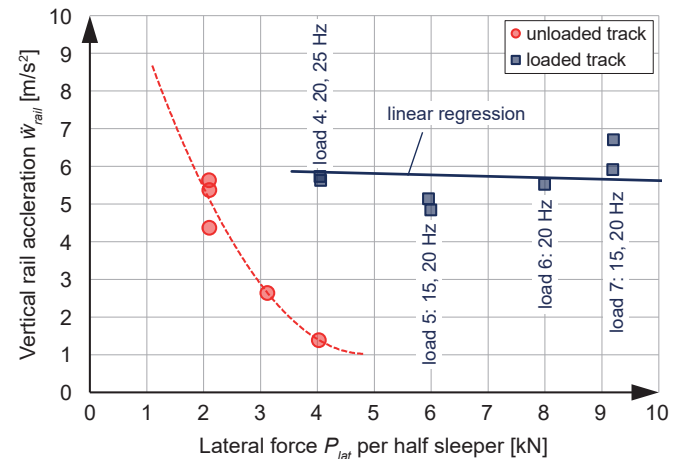


Fig. 8. Test principle 1 – load-dependent acceleration limits for lateral track resistance: comparison between loaded and unloaded track

To describe the limit states for the loaded track, linear regression is formulated (blue line in Fig. 8):

$$\ddot{w}_{rail,lim} = -0.038 P_{lat} + 6.0, [\text{m/s}^2]. \quad (2)$$

Fig. 8 thus illustrates that the vertical vibration state (unloaded vs loaded track) clearly influences lateral track resistance as a function of the lateral load (neglecting the excitation frequency). A significant loss of lateral track resistance – in this case defined by a disproportionate increase in lateral displacement – can already occur at accelerations below the limit value of  $3.5 \text{ m/s}^2$  according to EN 1990/A1 [1]. Lastly, it should be noted that the identified limit accelerations apply to a half-track section. This circumstance is further discussed in the final section 4.

### 3.2. ACCELERATION-DEPENDENT LATERAL TRACK RESISTANCE

Following the results of experiments according to principle 1, the results for principle 2 are presented in this subsection. In experiments according to principle 2, a stationary vibration state (constant vertical acceleration amplitude at a defined excitation frequency) is set, and then the lateral load  $P_{lat}$  is increased. As a result, Fig. 9 shows the measured force-displacement curves for different vibration states – defined by the vertical acceleration amplitude of the trough  $\dot{w}_{TR}$  – and two different vertical load states (loaded vs. unloaded track). The lateral force  $P_{lat}$  is related to the entire installed track (four half-sleepers). Fig. 9 shows both tests in the dynamic state (blue lines) and the static state (without dynamic vertical excitation – grey lines) for the loaded condition. Results for the loaded track show that lateral track resistance decreases significantly due to the vertical vibrations of the supporting structure (compare grey vs. blue lines), but the results agree well for accelerations between  $3 \text{ m/s}^2$  and  $6.7 \text{ m/s}^2$ . Vertical excitation of the superstructure thus reduces lateral track resistance, but there is no abrupt loss of stiffness in the analysed range.

Concerning the unloaded track condition (black dashed lines in Fig. 9), lateral track resistance is significantly lower compared to the vertically loaded condition. Furthermore, there is an evident influence of the vertical acceleration level. Generally speaking, lateral track resistance decreases with increasing acceleration.

As mentioned, the lateral load  $P_{lat}$  specified in Fig. 9 applies to the installed track section with four half-sleepers. To determine the lateral track resistance for a single whole sleeper, an approach has to be developed to divide the lateral resistance into individual components (distribution to individual mechanisms). Furthermore, as shown

in Fig. 2, the value of lateral load associated with relative displacement of  $2 \text{ mm}$  is used at this point as a reference for determining the values of lateral track resistance (red dashed line in Fig. 9). For an approach to distribute the lateral resistance to individual sub-mechanisms, the following percentage distribution is selected based on [9]:

- component 1 – bottom friction: 50%,
- component 2 – threshold flank resistance: 10%,
- component 3 – head resistance: 40%.

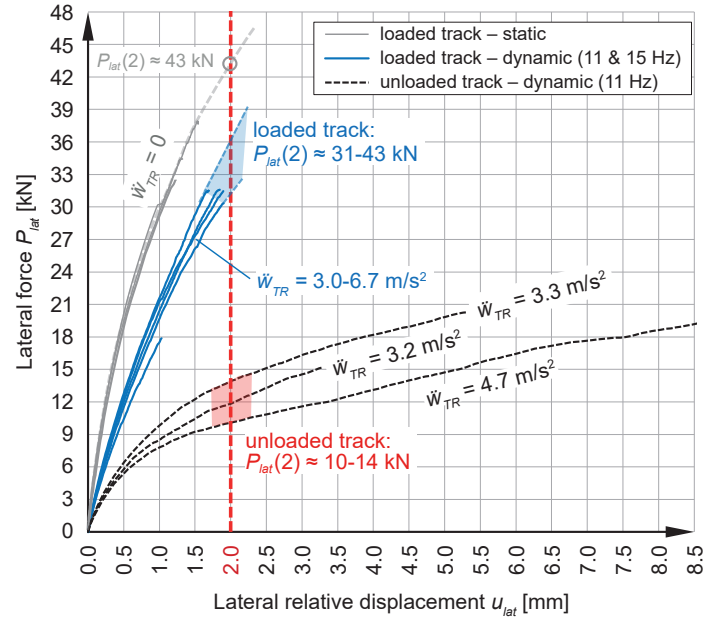


Fig. 9. Test principle 2 – lateral force-displacement curves depending on different acceleration levels: comparison between loaded and unloaded track

The experiments were carried out on half-track, each covering half of components 1 and 2 (friction between ballast and sleepers). In contrast, the experiments fully cover component 3 (shoulder contribution), as the shoulder resistance only occurs on one side of the track. Based on the selected percentage distribution, the lateral track resistances per sleeper in relation to a full track are calculated from the tests as follows:

$$P_{lat,full} = \frac{1}{4} (0.4 + 2 \cdot 0.6) P_{lat}(2), [\text{kN}]. \quad (3)$$

Equation (3) yields the following values for lateral track resistance of the vertically vibrating superstructure, related to a full section of ballast superstructure, independent of the excitation frequency:

- unloaded track:  $4.0 \leq P_{lat,full} \leq 5.6 \text{ kN/sleeper}$ ,
- loaded track:  $12.4 \leq P_{lat,full} \leq 14.4 \text{ kN/sleeper}$ .

These values can be used as an initial reference for assessing the track stability of railway bridges subjected to dynamic vibrations. Lateral stiffness for the unloaded track is used primarily to assess track stability in the event of combined loading from longitudinal stresses (e.g. due to temperature) and vertical vibrations (after train passage and without simultaneous vertical loading).

The results relate exclusively to the ballasted track; the properties of the bridge – such as the horizontal natural frequency – remain unaffected. The results are also independent of the bridge type and apply to all types of construction (steel, concrete, composite and filler beam bridges). Concerning possible long-term effects, the experiments presented here did not explicitly investigate such effects. However, studies in [24] have shown that the stiffness behaviour of ballast at the beginning and end of its lifecycle differs only to a marginal extent, which is therefore negligible.

#### 4. CONCLUSIONS AND OUTLOOK

The experimental investigations of lateral track resistance under the influence of vertical vibrations presented in this contribution as an isolated analysis of a section of ballast superstructure provide essential findings on the dynamic behaviour of ballast superstructures on railway bridges. Through its specialised design and functional principle, the large-scale test facility enables an isolated and targeted investigation of a representative section of ballast superstructure at the scale of 1:1, whereby two different test principles are used for the qualitative and quantitative assessment of lateral track resistance influenced by vertical vibrations. The summarised conclusions are as follows:

1. The limit values for vertical acceleration identified based on principle 1 (constant lateral force and successive increase in vertical acceleration), above which a noticeable decrease in lateral track resistance occurs, are important indicators for the condition assessment of railway bridges, enabling assessment of track stability under dynamic excitation. In particular, the identified load-dependent acceleration limits shown in Fig. 8 should be perceived in the context of the currently valid limit values according to EN 1990/A1 [1] and are regarded as qualitative reference values due to the half-section investigated. Nevertheless, the investigations show that changes in ballast superstructure behaviour can already occur at vertical acceleration levels below  $3.5 \text{ m/s}^2$  for unloaded track.

2. The excitation frequency does not noticeably influence the identified acceleration limits. This frequency-independent stiffness behaviour has already been observed based on experiments for horizontal and vertical track-bridge interaction [19-21] and, therefore, also applies to the lateral track-bridge interaction discussed in this contribution.
3. Based on the tests according to principle 2 (increasing lateral load at constant vertical acceleration), it was possible to determine values of track resistance for both the unloaded and loaded condition using an approach for distributing the lateral track resistance to individual sub-mechanisms.
4. Regarding lateral stiffness, the vertical acceleration level influences lateral track resistance, especially in the case of unloaded track (Fig. 9).

The findings presented in this contribution on lateral track resistance and its behaviour under dynamic excitation in the form of vertical vibrations can subsequently be included in dynamic analyses for condition assessment of railway bridges and assessing track stability.

Further investigations will involve statistical validation of the findings and their comparison with computer simulations. These analyses will be based on data created as part of the experiments presented in this contribution. Furthermore, the conclusions of the experiments on lateral track-bridge interaction suggest that the currently defined vertical limit accelerations according to EN 1990/A1 [1] and B 4008-2 [2] may need to be reconsidered. However, further investigations and experiments are required in this context to create a more comprehensive database.

#### ACKNOWLEDGEMENTS

The research presented in this contribution was funded by the Austrian Federal Railways (ÖBB Infrastruktur AG) in relation to the research project “DynSchoStab” (acronym). The authors would like to sincerely thank ÖBB Infrastruktur AG for their support.

## REFERENCES

- [1] EN 1990/A1:2013 05 15 Eurocode – Basis of structural design – Amendment 1: Application for bridges (consolidated version). Austrian Standards International, Vienna
- [2] ÖNORM B 4008-2:2019 11 15 Assessment of load capacity of existing structures – Part 2: bridge construction. Austrian Standards International, Vienna
- [3] ERRI D214 Railway bridges for speeds > 200 km/h, RP 2 – RP 9. European Rail Research Institute, 1999, Utrecht
- [4] *Zhai W., Han Z., Chen Z., Ling L., Zhu S.*: Train-track-bridge dynamic interaction: a state-of-the-art review. *Vehicle System Dynamics*, **57**, 7, 2019, 984-1024, DOI: 10.1080/00423114.2019.1605085
- [5] *Ticona Mela L.R., Ribeiro D., Calçada R., Bittencourt T.N.*: Validation of a vertical train-track-bridge dynamic interaction model based on limited experimental data. *Structure and Infrastructure Engineering*, **16**, 1, 2020, 181-201, DOI: 10.1080/15732479.2019.1605394
- [6] *Yang B., Yau J.D., Wu Y.S.*: Vehicle-bridge interaction dynamics with applications to high-speed railways. World Scientific, Taipei, 2004
- [7] *Bettinelli L., Stollwitzer A., Fink J.*: Numerical study on the influence of coupling beam modeling on structural accelerations during high-speed train crossings. *Applied Sciences*, **13**, 15, 2023, Article ID: 8746, DOI: 10.3390/app13158746
- [8] *Atapin V., Bondarenko A., Sysyn M., Grün D.*: Monitoring and evaluation of the lateral stability of CWR track. *Journal of Failure Analysis and Prevention*, **22**, 2022, 319-332, DOI: 10.1007/s11668-021-01307-3
- [9] *Hasan N.*: Buckling of a ballasted curved track under unloaded conditions. *Advances in Mechanical Engineering*, **13**, 6, 2021, DOI: 10.1177/168781402111025187
- [10] *Lichtberger B.*: Handbuch Gleis – Unterbau, Oberbau, Instandhaltung, Wirtschaftlichkeit. Tetzlaff Verlag, Hamburg, 2010
- [11] *Wang H., Xing C., Deng X.*: Effect of Random Lateral Ballast Resistance on Force-Deformation Characteristics of CWR with a Small-Radius Curve. *Materials*, **16**, 7, 2023, Article ID: 2876, DOI: 10.3390/ma16072876
- [12] *Khatibi F., Esmaeili M., Mohammadzadeh S.*: DEM analysis of railway track lateral resistance. *Soils and Foundations*, **57**, 4, 2017, 587-602, DOI: 10.1016/j.sandf.2017.04.001
- [13] *Esmaeili M., Hosseini S.A.S., Sharavi M.*: Experimental assessment of dynamic lateral resistance of railway concrete sleeper. *Soil Dynamics and Earthquake Engineering*, **82**, 2016, 40-54, DOI: 10.1016/j.soildyn.2015.11.011
- [14] *Mohammadzadeh S., Esmaeili M., Khatibi F.*: A new field investigation on the lateral and longitudinal resistance of ballasted track. *Proceedings of the Institution of Mechanical Engineers, Part F: Journal of Rail and Rapid Transit*, **232**, 8, 2018, 2138-2148, DOI: 10.1177/0954409718764190
- [15] *Jing A., Aela P.*: Review of the lateral resistance of ballasted tracks. *Proceedings of the Institution of Mechanical Engineers, Part F: Journal of Rail and Rapid Transit*, **234**, 8, 2020, 807-820, DOI: 10.1177/0954409719866355
- [16] *Zakeri J.A.*: Lateral Resistance of Railway Track. In: *Reliability and Safety in Railway*, IntechOpen, Rijeka, 2012, 354-378, DOI: 10.5772/35421
- [17] *Jing G., Aela P., Fu H.*: The contribution of ballast layer components to the lateral resistance of ladder sleeper track. *Construction and Building Materials*, **202**, 2019, 796-805, DOI: 10.1016/j.conbuildmat.2019.01.017
- [18] *Le Pen L.M., Powrie W.*: Contribution of base, crib and shoulder ballast to the lateral sliding resistance of railway track: a geotechnical perspective. *Proceedings of the Institution of Mechanical Engineers, Part F: Journal of Rail and Rapid Transit*, **225**, 2, 2011, 113-128, DOI: 10.1177/0954409710397094
- [19] *Stollwitzer A., Bettinelli L., Fink J.*: The longitudinal track-bridge interaction of ballasted track in railway bridges: Experimental determination of dynamic stiffness and damping characteristics. *Engineering Structures*, **274**, 2023, Article ID: 115115, DOI: 10.1016/j.engstruct.2022.115115
- [20] *Stollwitzer A., Bettinelli L., Fink J.*: Experimental analysis of longitudinal and lateral track-bridge interaction of the ballasted track in railway bridges. *2nd Conference of the European Association on Quality Control of Bridges and Structures EUROSTRUCT 2023, ce/papers*, **6**, 5, 2023, 430-439, DOI: 10.1002/cepa.2128
- [21] EN 1991-2:2012 03 01 Eurocode 1: Actions on structures – Part 2: Traffic loads on bridges (consolidated version). Austrian Standards International, Vienna
- [22] *Stollwitzer A., Bettinelli L., Fink J.*: Vertical track-bridge interaction in railway bridges with ballast superstructure: experimental analysis of dynamic stiffness and damping behavior. *International Journal of Structural Stability and Dynamics*, DOI: 10.1142/S0219455425400085
- [23] *Stollwitzer A., Fink J.*: Dämpfungskennwerte des Schotteroberbaus auf Eisenbahnbrücken, Teil 2: Energiedissipation im Schotteroberbau und zugehöriges Rechenmodell. *Bau-technik*, **98**, 8, 2021, 552-562, DOI: 10.1002/bate.202000100 (in German)
- [24] *Hackl K.*: Development and application of a testing facility for studying the dynamic behaviour of ballasted track at railway bridges. *repositUM: Dissertation, Technische Universität Wien*, 2017, DOI: 10.34726/hss.2017.50541 (in German)